

Supporting Information

Solid-liquid equilibria of binary mixtures of fluorinated ionic liquids

Ana Rita R. Teles^a, Helga Correia^a, Guilherme J. Maximo^b, Luís P. N. Rebelo^c, Mara G. Freire^a, Ana B. Pereiro^{c*} and João A. P. Coutinho^a

^a CICECO - Aveiro Institute of Materials, Department of Chemistry, University of Aveiro, 3810-193 Aveiro, Portugal.

^b Laboratory of Extraction, Applied Thermodynamics and Equilibrium, School of Food Engineering, University of Campinas, Campinas, São Paulo, Brazil

^c Instituto de Tecnologia Química e Biológica António Xavier (www.itqb.unl.pt), UNL, Av. República, Apartado 127, 2780-901 Oeiras, Portugal.

Table S1. Experimental data for the melting temperatures, enthalpies of fusion, transition temperatures, and enthalpies of transition for the system x [C₄C₁pyr] [N(C₄F₉SO₂)₂] + (1- x) [C₄C₁pyr] [C₄F₉SO₃].

$x_{[\text{C}_4\text{C}_1\text{pyr}][\text{N}(\text{C}_4\text{F}_9\text{SO}_2)_2]}$	$T_{\text{fus}} / \text{K}$	$\Delta_{\text{fus}}H / \text{kJ}\cdot\text{mol}^{-1}$	T_{Tr1}/K	$\Delta_{\text{Tr1}}H/\text{kJ}\cdot\text{mol}^{-1}$
0.00	361	13	-	-
0.07	358	21	-	-
0.17	348	12	305	1.9
0.29	334	6.3	307	3.3
0.38	323	2.0	305	5.9
0.48	312	0.28	306	9.2
0.59	315	0.22	306	7.2
0.69	332	2.6	305	2.9
0.74	339	1.7	305	1.8
0.79	348	2.6	-	-
0.84	356	4.7	-	-
0.89	363	5.5	-	-
0.93	368	7.6	-	-
1.00	374	6.0	-	-

Table S2. Experimental data for the melting temperatures, enthalpies of fusion, transition temperatures, and enthalpies of transition for the system x [C₂C₁pyr] [N(C₄F₉SO₂)₂] + (1- x) [C₂C₁pyr] [CF₃SO₃].

$x_{[\text{C}_2\text{C}_1\text{pyr}][\text{N}(\text{C}_4\text{F}_9\text{SO}_2)_2]}$	$T_{\text{fus}} / \text{K}$	$\Delta_{\text{fus}}H/\text{kJ}\cdot\text{mol}^{-1}$	T_{Tr1}/K	$\Delta_{\text{Tr1}}H/\text{kJ}\cdot\text{mol}^{-1}$
0.00	384	6.7	-	-
0.09	372	18	355	6.9
0.21	365	8.5	357	13
0.27	361	5.0	357	17
0.33	360	1.8	357	18
0.38	357	18	357	18
0.46	365	2.5	356	15
0.59	377	6.2	356	10
0.67	387	2.8	355	6.1
0.77	399	3.6	353	4.1
0.89	417	2.7	348	0.54
1.00	431	7.9	-	-

Table S3. Experimental data for the melting points and enthalpies of fusion for the system x [C₄C₁pyr] [N(C₄F₉SO₂)₂] + (1-x) [C₂C₁pyr] [N(C₄F₉SO₂)₂].

$x_{[\text{C}_4\text{C}_1\text{pyr}][\text{N}(\text{C}_4\text{F}_9\text{SO}_2)_2]}$	T_{fus}/K	$\Delta_{\text{fus}}H/\text{kJ}\cdot\text{mol}^{-1}$
0.00	431	16
0.10	425	16
0.24	411	14
0.39	401	13
0.49	395	13
0.59	391	13
0.74	384	12
0.89	380	12
1.00	373	12

Table S4. Experimental data for the melting temperatures, enthalpies of fusion, transition temperatures, and enthalpies of transition for the system x [C₄C₁pyr] [C₄F₉SO₃] + (1-x) [N_{1112(OH)}] [C₄F₉SO₃].

$x_{[\text{C}_4\text{C}_1\text{pyr}][\text{N}(\text{C}_4\text{F}_9\text{SO}_2)_2]}$	T_{fus}/K	$\Delta_{\text{fus}}H/\text{kJ}\cdot\text{mol}^{-1}$	T_{Tr1}/K	$\Delta_{\text{Tr1}}H/\text{kJ}\cdot\text{mol}^{-1}$	T_{Tr2}/K	T_{Tr3}/K
0.00	449	3.7	-	1.4	406	378
0.06	436	7.2	367	2.1	408	373
0.09	429	6.1	360	2.9	406	374
0.15	417	2.3	358	3.0	404	-
0.21	403	1.7	358	1.7	-	371
0.22	400	1.4	356	1.4	-	374
0.24	400	1.2	359	1.1	-	375
0.28	390	4.9	359	5.6	-	379
0.32	378	6.8	358	0.92	-	-
0.38	377	7.6	358	1.8	-	-
0.48	378	9.8	361	1.7	-	-
0.58	377	12	364	2.2	-	-
0.68	377	13	365	3.9	-	-
0.78	374	18	361	3.2	-	-
0.85	369	19	356	5.4	-	-
0.94	361	20	-	-	-	-
1.00	361	25	-	-	-	-

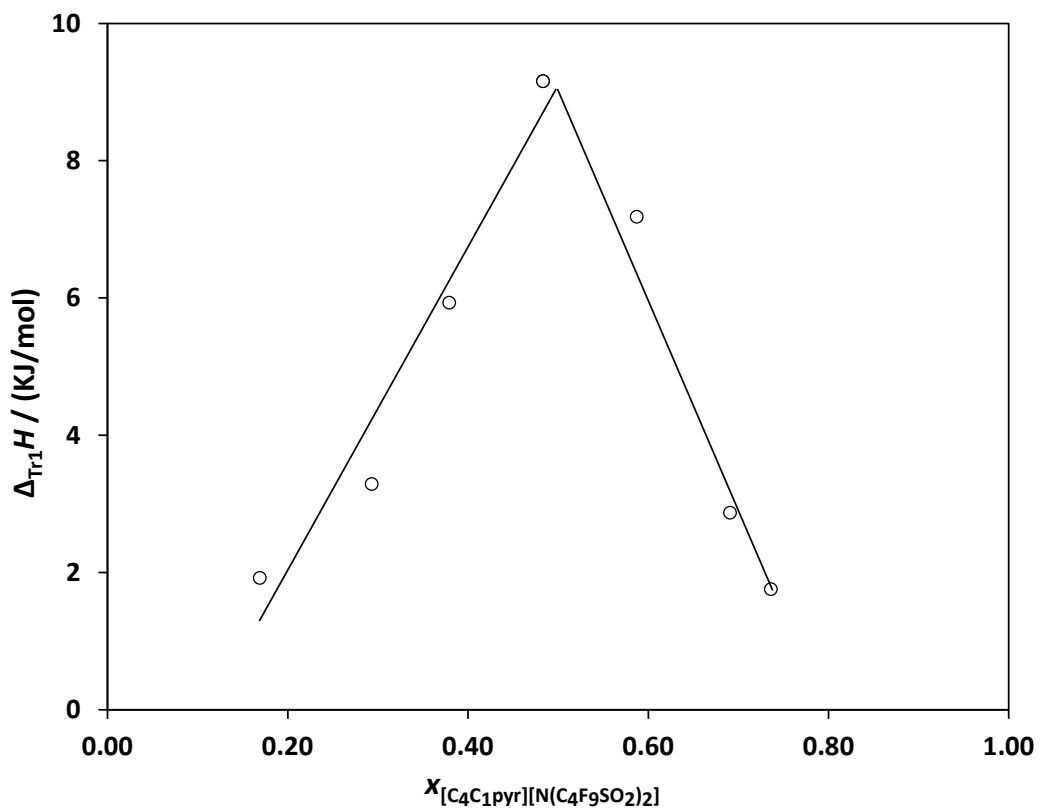


Fig.S1. Tamman plot for the binary system $x [C_4C_1\text{pyr}] [N(C_4F_9\text{SO}_2)_2] + (1-x) [C_4C_1\text{pyr}] [C_4F_9\text{SO}_3]$: (○) enthalpy of the eutectic transition, $\Delta_{Tr1}H$, versus mole fraction of $[C_4C_1\text{pyr}] [N(C_4F_9\text{SO}_2)_2]$. Solid lines represent linear fits to the enthalpy values.

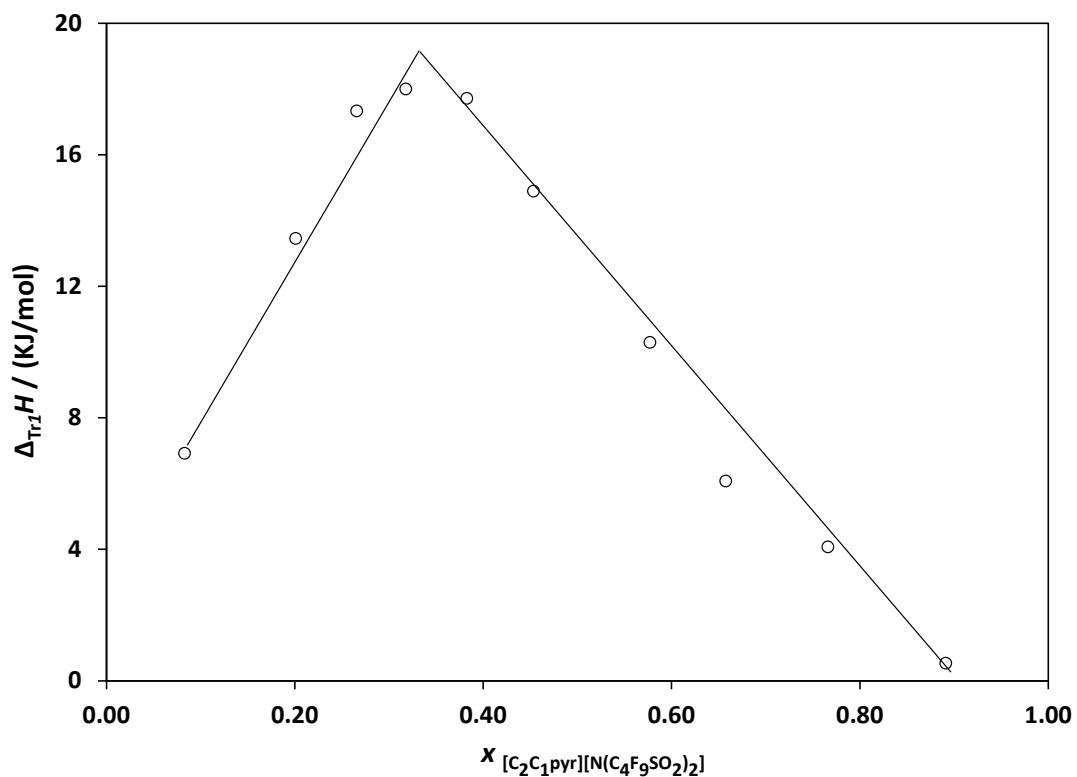


Fig.S2. Tamman plot for the binary system $x [C_2C_1\text{pyr}] [N(C_4F_9\text{SO}_2)_2] + (1-x) [C_2C_1\text{pyr}] [CF_3\text{SO}_3]$: (○) enthalpy of the eutectic transition, $\Delta_{Tr1}H$, versus mole fraction of $[C_2C_1\text{pyr}] [N(C_4F_9\text{SO}_2)_2]$. Solid lines represent linear fits to the enthalpy values.

Viscosity and density measurements

Experimental methods

Viscosity and density measurements of mixtures composed of [C₄C₁pyr] [N(C₄F₉SO₂)₂] + [C₄C₁pyr] [C₄F₉SO₃] with mole fraction of 0.40, 0.50 and 0.60, were performed in the temperature range between 328.15 and 363.15 K, at atmospheric pressure, using an automated SVM 3000 Anton Paar rotational Stabinger viscometer-densimeter. The SVM 3000 uses Peltier elements for fast and efficient thermostability. The relative uncertainty for the dynamic viscosity values is 0.5 % and the absolute uncertainty for the density values is 0.0005 g·cm⁻³.

Results and discussion

The density and dynamic viscosity of mixtures close to the eutectic point for the binary system [C₄C₁pyr] [N(C₄F₉SO₂)₂] + [C₄C₁pyr] [C₄F₉SO₃] were determined, at atmospheric pressure and as a function of temperature, in order to better characterize this mixture. The experimental results are reported in Table S5 of ESI and displayed in Figure S3. The molar volumes for these mixtures were also calculated from density data and are plotted in Figure S4.

These measurements show that the increment of the amount of [C₄C₁pyr] [N(C₄F₉SO₂)₂] for a specific temperature implies an increment in both the density and molar volume, and a decrease in the viscosity. It is important to note that, generally, the mixing of two ionic liquids involves the mixing of four ions (in this case only three ions because this mixture has a common ion, the [C₄C₁pyr]⁺ cation). Therefore, the mixtures' physical properties reflect the amounts present of different chemical moieties, in this case the presence of either the [N(C₄F₉SO₂)₂]⁻ or the [C₄F₉SO₃]⁻ anion. The incorporation of the [N(C₄F₉SO₂)₂]⁻ anion increases the volume of the fluorinated domains in the binary mixture, thus causing a decrease in the intensity of the Coulombic interactions. These facts might justify the decrease of the dynamic viscosity with the increasing incorporation of this anion. Furthermore, the greater number of fluor atoms causes an increment in the density and also justifies the increment of molar volume when the amount of [C₄C₁pyr] [N(C₄F₉SO₂)₂] increases. The number of fluor atoms and the volume of the [N(C₄F₉SO₂)₂]⁻ anion is obviously higher than that of the [C₄F₉SO₃]⁻ anion.

Table S5. Experimental data for the viscosity and density measurements for the system [C₄C₁pyr] [N(C₄F₉SO₂)₂] + [C₄C₁pyr] [C₄F₉SO₃] in the eutectic region.

T/ K	X _{[C₄C₁pyr][N(C₄F₉SO₂)₂]} = 0.38		X _{[C₄C₁pyr][N(C₄F₉SO₂)₂]} = 0.48		X _{[C₄C₁pyr][N(C₄F₉SO₂)₂]} = 0.59	
	η / mPa·s	ρ / g·cm ⁻³	η / mPa·s	ρ / g·cm ⁻³	η / mPa·s	ρ / g·cm ⁻³
328.15	147.1	1.4662	155.3	1.4848	143.8	1.4972
333.15	115.2	1.4613	121.5	1.4795	113.2	1.4918
338.15	91.59	1.4564	96.55	1.4742	89.99	1.4864
343.15	73.87	1.4515	77.55	1.4690	72.67	1.4811
348.15	60.28	1.4466	63.17	1.4639	59.42	1.4758
353.15	49.78	1.4417	52.06	1.4588	43.19	1.4706
358.15	41.50	1.4369	43.34	1.4538	36.02	1.4655
363.15	34.97	1.4321	36.42	1.4489	30.28	1.4604

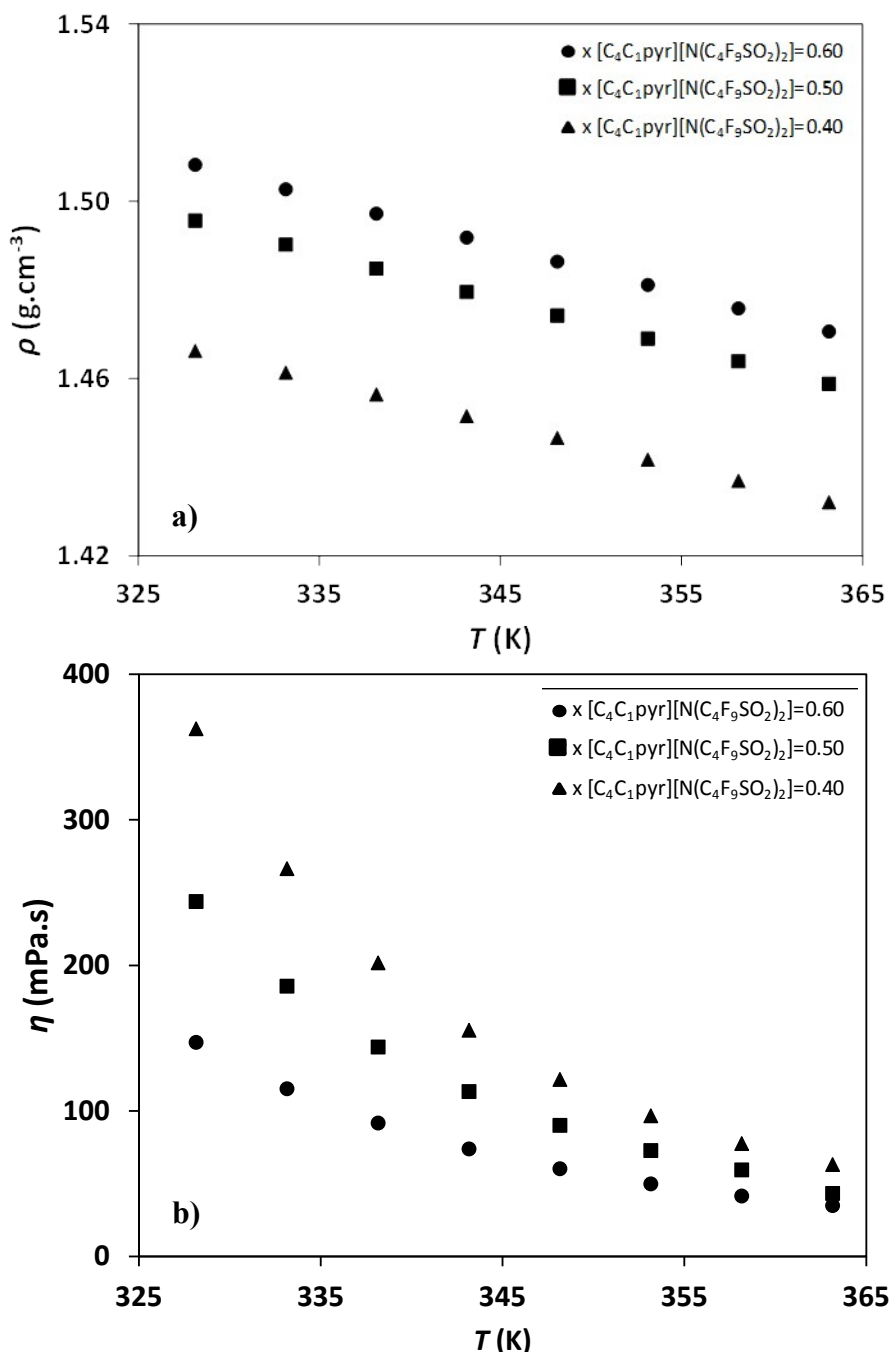


Fig. S3. Density and dynamic viscosity of some mixtures close to the eutectic region for the binary system x $[C_4C_1\text{pyr}] [N(C_4F_9SO_2)_2] + (1-x) [C_4C_1\text{pyr}] [C_4F_9SO_3]$.

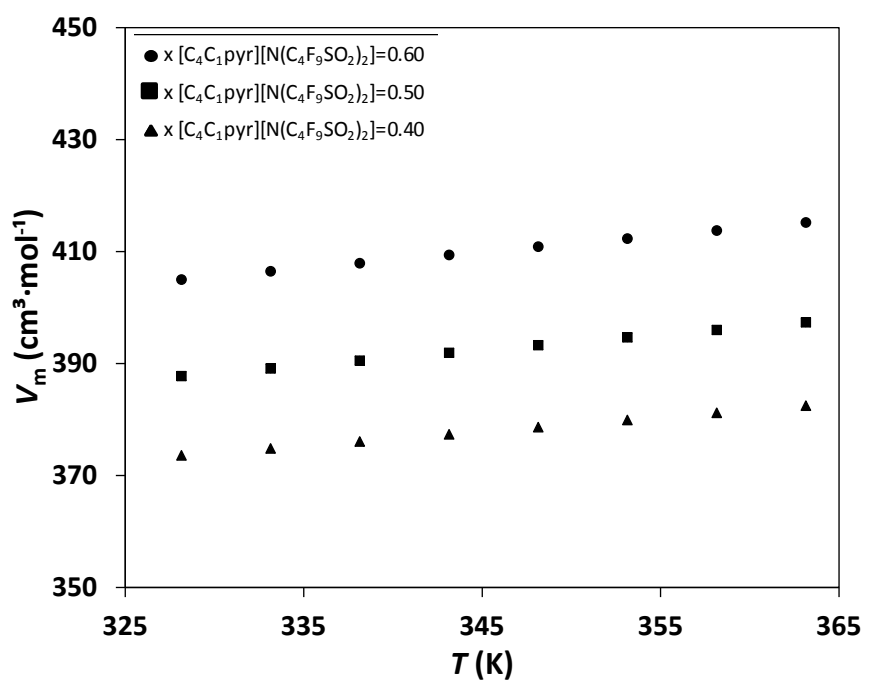


Fig. S4. Molar volume of some mixtures in the eutectic region for the system $x [C_4C_1\text{pyr}][N(C_4F_9SO_2)_2] + (1-x) [C_4C_1\text{pyr}][C_4F_9SO_3]$.

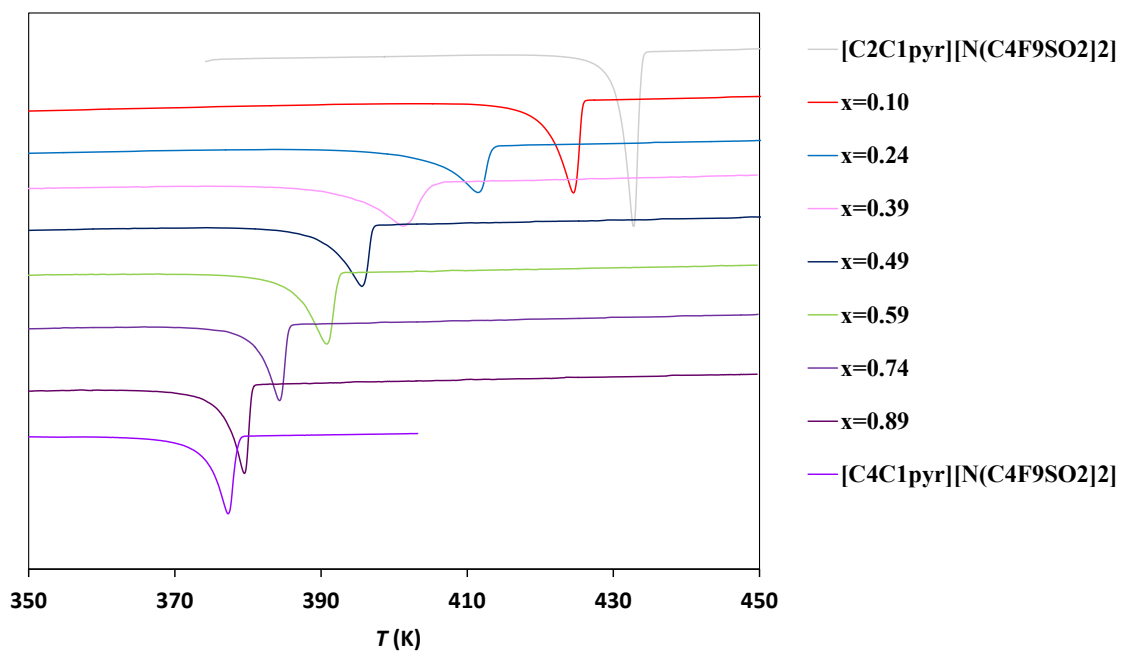


Fig. S5. DSC thermograms (heating run) for the binary mixture x [C₄C₁pyr] [N(C₄F₉SO₂)₂] + (1- x) [C₂C₁pyr] [N(C₄F₉SO₂)₂].